

Refinement of Nb₃Sn grain size by the generation of ZrO₂ precipitates in Nb₃Sn wires

X. Xu,^{1,a)} M. Sumption,¹ X. Peng,² and E. W. Collings¹

¹*Department of Materials Science and Engineering, the Ohio State University, Columbus, OH43210, USA*

²*Hyper Tech Research Incorporated, 539 Industrial Mile Road, Columbus, OH 43228, U.S.A*

In this letter we demonstrate that if oxygen can be properly supplied to (Nb-Zr)-Sn wires, ZrO₂ precipitates will form during the heat treatment, refining the Nb₃Sn grain size markedly. Here, a Nb₃Sn subelement was fabricated in which Nb-1Zr alloy was used, and oxygen was supplied via SnO₂ powder. The results showed that such a design could supply sufficient oxygen to internally oxidize the Zr in the Nb-1Zr alloy, and that the sample reacted at 650 °C had grain sizes of ~45 nm, less than half the size of the grains in present Nb₃Sn conductors. Magnetic measurements showed that the peak of the pinning force vs. field (F_p - B) curve was shifted to $\sim 0.3B_{irr}$ (the irreversibility field).

Nb₃Sn superconductors are of significant interest for applications in particle accelerators, undulators, fusion reactor designs, nuclear magnetic resonance (NMR) machines, and research magnets.¹ The planned upgrade of the interaction region magnets of the Large Hadron Collider (LHC) to meet the goal of higher luminosity requires Nb₃Sn conductors of high performance, especially high critical current density J_c at up to 15 T.²

Improvement of the high field J_c of Nb₃Sn conductors can be realized in two ways: increasing the irreversibility field (B_{irr}) and enhancing the pinning capacity. The potential for the improvement in the B_{irr} of Nb₃Sn conductors is limited, as the B_{irr} s of the state-of-the-art Nb₃Sn strands at 4.2 K are normally 24-26 T,³⁻⁵ which is quite close to the limit of the upper critical field (B_{c2}) of ternary Nb₃Sn, ~ 27 T at 4.2 K (which corresponds to ~ 31 T at 0 K).⁶ The greatest potential for Nb₃Sn conductor development, on the other hand, lies in improving the pinning capacity. It has long been recognized that grain boundaries are the main flux line pinning centers in Nb₃Sn. Present Nb₃Sn conductors, with grain sizes of typically 100-200 nm, follow flux shear behavior, illustrated by the fact that the bulk pinning force vs. field (F_p - B) curve peaks at $0.2B_{irr}$.⁷ Dieterich's experiment⁸ on Nb₃Sn films fabricated by electron-beam co-evaporation showed that if the Nb₃Sn grain size is refined to 15-30 nm, the peak of the F_p - B curve could be shifted from $0.2B_{irr}$ to $0.5B_{irr}$, which can improve the 12 T J_c by a factor of three.⁸

^{a)} Author to whom correspondence should be addressed. Electronic mail: xu.452@osu.edu.

The primary method that has been used to control the Nb_3Sn grain size has been lowering the reaction temperature. However, further lowering of the reaction temperature relative to the current level (625-650 °C) is inadvisable as it drives the Nb_3Sn phase off-stoichiometry and also requires excessive

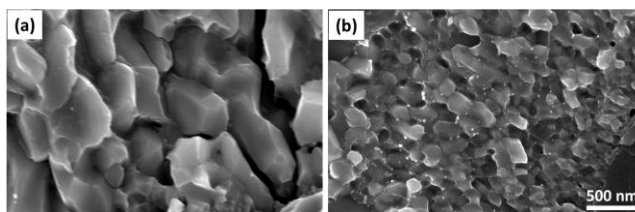


Fig. 1. Fracture SEM images of type A samples reacted at 850 °C for 10 min in (a) pure argon and (b) argon-oxygen atmospheres.

reaction time. On the other hand, the internal oxidation method that was successfully used in Nb_3Sn films⁹ offers an alternative. The film approach used a Nb-Zr foil into which oxygen was supplied by anodization and subsequent annealing; after being coated with Cu-Sn, the foil was reacted at 1050 °C to form Nb_3Sn with ZrO_2 precipitates. It was reported that with sufficient oxygen content, the Nb_3Sn grain size could be refined by an order of magnitude.⁹

Transferring this method to Nb_3Sn wires, however, has not yet been realized, mainly because pre-dissolving oxygen in Nb-Zr markedly increases its strength and decreases its ductility, making the wires hard to process. To circumvent the usage of the Nb-O alloy, Zeitlin added SnO_2 powder into the Sn core of a mono-element internal-tin strand, expecting the Nb-Zr to reduce SnO_2 during heat treatment and take up the oxygen,¹⁰ because according to the Ellingham diagram, Nb and Zr have much stronger affinity to oxygen than does Sn. However, no grain refinement was observed in his samples reacted at or below 850 °C.

To find out whether this was due to a defect in the experimental design or alternatively because generating ZrO_2 precipitates in Nb_3Sn wires is inherently impossible at low reaction temperatures, we fabricated a series of composites, starting with a Nb-1Zr alloy tube surrounding a Cu/Sn core, here denoted composite A. With such a design the Nb-1Zr alloy was exposed to the atmosphere during heat treatment, so oxygen could be supplied to the Nb-1Zr externally. For comparison various samples were given the same heat treatments in pure argon and in argon-oxygen atmospheres at various temperatures from 650 to 850 °C.

Fracture scanning electron microscopy (SEM) images of the samples reacted at 850 °C without and with oxygen are shown in Fig. 1. It is clear that the grain size of the sample reacted in argon-oxygen atmosphere is substantially smaller. From the transmission electron microscopy (TEM) image shown in Fig. 2, we can clearly see intra-granular ZrO_2

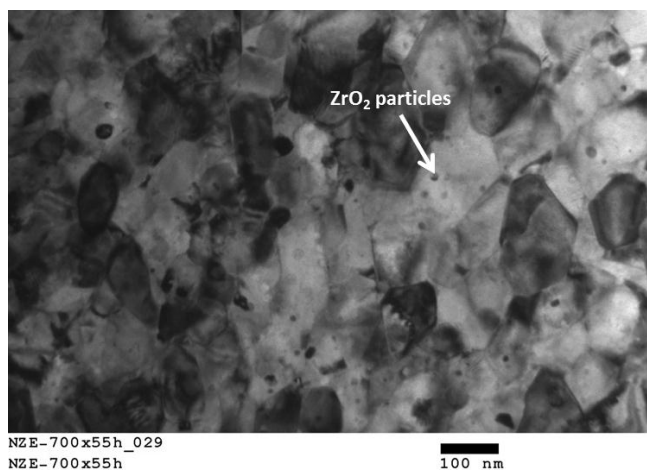


Fig. 2. TEM image of sample A reacted at 700 °C for 55 hours in an argon-oxygen atmosphere. An example of a ZrO_2 particle is marked.

particles of various sizes.⁹ Fig. 3 presents the dependence of Nb₃Sn grain size for type A samples on reaction temperature. The grain sizes were calculated by the method described in Ref. 11. At all of the investigated temperatures the grain sizes of the samples reacted in argon-oxygen mixtures are much smaller than those reacted in the absence of oxygen. Similar to standard Nb₃Sn strands, ZrO₂ stabilized Nb₃Sn grains become smaller as the reaction temperature is reduced. We also noticed that for the samples containing ZrO₂ there is a grain size gradient across the Nb₃Sn layer. For example, the grain size of the sample reacted at 650 °C changes from ~55 nm near the Cu-Sn core to ~40 nm near the unreacted Nb.

Since grain size variations across the Nb₃Sn layers in standard Nb₃Sn wires are typically small (excluding cases where grain morphology changes),¹² we think this grain size gradient could be due to an oxygen concentration gradient across the Nb-1Zr layer prior to Nb₃Sn formation. One possible mechanism of the grain refinement due to the formation of ZrO₂ particles was proposed by Rumaner *et al.*⁹: Zr and O dissolve readily into Nb, but have limited solubility in Nb₃Sn, so during the Nb₃Sn layer growth they are expelled and precipitated out as fine ZrO₂ particles. The ZrO₂ precipitates are coherent with the host Nb₃Sn lattice and can inhibit the Nb₃Sn grain boundaries from migrating.

The above study demonstrates that ZrO₂ precipitates can form and the grain size can be refined in (Nb-Zr)₃Sn strands provided that sufficient oxygen is absorbed by Nb-Zr before it is transformed to Nb₃Sn. Returning to Zeitlin's study, we speculate that the reason why no grain refinement occurred was that the intact Cu layer that surrounded the Sn+SnO₂ core in his conductor¹⁰ had, according to the Ellingham diagram, a lower affinity to oxygen than did Sn, thus prevented SnO₂ from being reduced. In other words, the "inert" Cu layer blocked the path of oxygen transfer. It should then be possible to inject oxygen from within the composite, as long as the SnO₂ powder reaches the Nb-Zr directly, without the intervening copper (itself needed for A15 formation). To verify the feasibility of this approach, we fabricated a second composite, denoted B, by filling SnO₂ powder into a Cu encased Nb tube and drawing it down to 0.7 mm diameter, and subsequently reacted several segments at various temperatures. The oxygen content in the Nb was determined by measurement of the critical temperature (T_c): according to previous work,^{13, 14} the T_c of Nb drops by about 0.93 K for each 1 at.% O dissolved in Nb. The magnetic moment vs. temperature ($m-T$) curves for the samples after various heat treatments are shown in Fig. 4(a). It can be seen that

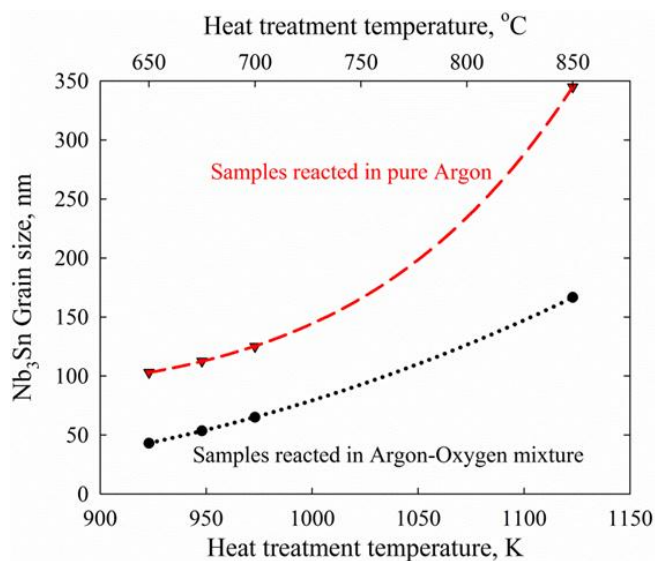


Fig. 3. Average Nb₃Sn grain size as a function of reaction temperature for type A samples reacted in pure argon and in argon-oxygen atmospheres. The dashed lines are exponential fits to the data.

the oxygen content increases with reaction temperature – which could be because of either increased absorption rate or increased oxygen solubility in Nb with temperature, reaching about 2 at.% for the sample reacted at 500 °C. It is also interesting to note that for the samples reacted at and above 550 °C, NbO₂ and NbO compounds formed after a certain reaction time, an example shown in Fig. 4 (b). We speculate

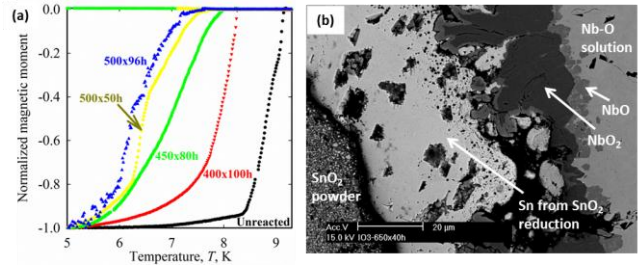


Fig. 4. (a) M - T curves of samples B reacted at various temperatures, and (b) SEM image of sample B reacted at 650 °C for 40 h, showing the Nb-O compounds.

that due to excessive SnO₂ amount in this composite B, as the oxygen content in the Nb saturated, Nb-O compounds began to form. Thus, this study warns against using excessive SnO₂ for oxygen supply.

With the knowledge that it is feasible to use SnO₂ powder as the oxygen source, we then fabricated a third composite, denoted C, along this line, by filling a Nb-1Zr tube with a Sn/Cu/SnO₂ tubular layer structure (that is, the SnO₂ powder is positioned between the Cu/Sn core and the Nb-1Zr tube wall), as shown in Fig. 5. For comparison purposes, we also fabricated an analog, D, with NbO₂ powder instead of SnO₂, and both were reacted at 650 °C for 150 h. The fracture SEM images of the reacted samples are shown in Fig. 6. The average grain sizes of samples C (with SnO₂) and D (with NbO₂) are

43 nm and 91 nm, respectively. In sample C there are a large fraction of grains with size smaller than 30 nm. The magnetic moment vs. temperature (m - T) curves in Fig. 7 (a) shows that the T_c of the unreacted Nb-1Zr in sample D is 9.1 K, whereas the value for sample C is 6.6 K, indicating that the NbO₂ powder failed to supply much oxygen, while in sample C nearly 3 at.% oxygen was absorbed by the Nb-1Zr alloy. Magnetic moment versus field measurements at 4.2 K (in the perpendicular direction) were performed on the reacted samples, and magnetic Nb₃Sn layer J_c s were calculated. The F_p - B curves for both samples are shown in Fig. 7 (b). The curves were fitted to the universal scaling law: $F_p = Kb^p(1-b)^q$, where K is a pre-factor related to the maximum pinning force $F_{p,max}$, and $b = B/B_{irr}$. The fitted B_{irr} values of samples C and D

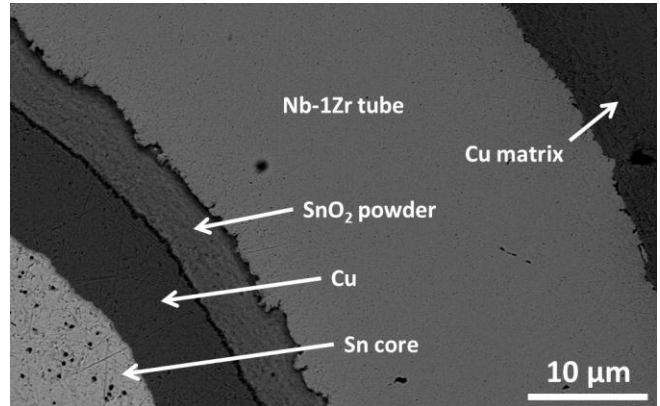


Fig. 5. SEM image of composite C. The black dots in the Sn core are due to polishing.

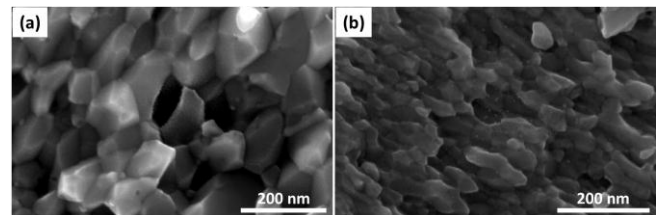


Fig. 6. Fracture SEM images of (a) sample D (with NbO₂) and (b) sample C (with SnO₂) reacted at 650 °C for 150 h.

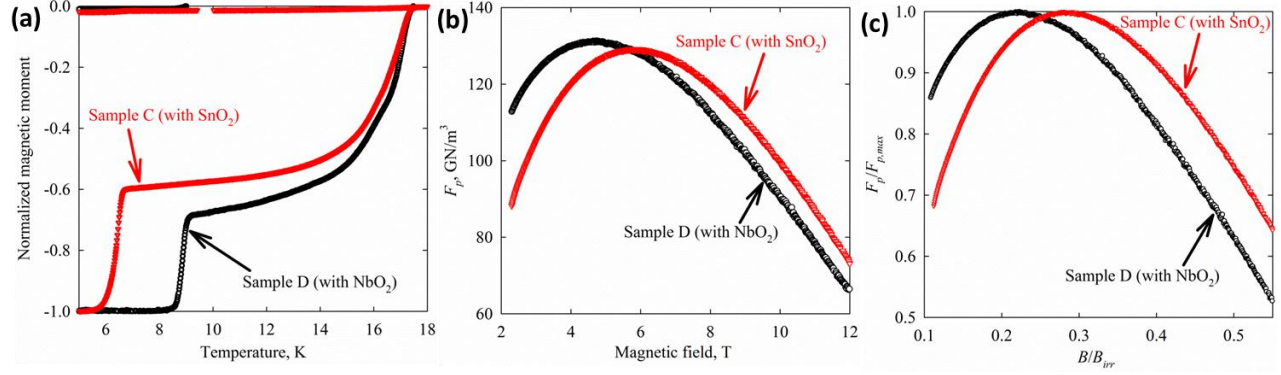


Fig. 7. The (a) m - T , (b) F_p - B , and (c) reduced F_p - B curves of samples D and C reacted at 650 °C for 150 h.

are respectively 20.5 and 21.3 T, relatively low because the samples were based on binary Nb₃Sn and were under-reacted.¹⁵ Fig. 7 (c) presents the $F_p/F_{p,max}$ vs. B/B_{irr} curves of samples C and D, peaking at $\sim 0.3B_{irr}$ and $\sim 0.2B_{irr}$, respectively. Sample D more or less follows the typical flux shear behavior; for sample C, on the other hand, an apparent shift of the F_p - B curve to higher field is observed. The high fraction of grains with size of sub-30 nm in sample C perhaps accounts for the shift of the F_p - B curve. It is interesting to note from Fig. 7 (b) that although sample C has smaller grain size, its $F_{p,max}$ is smaller than that of sample D. Similar phenomenon is also seen in the data of Dieterich's thin films.⁸ Possibly this is because sample D has higher upper critical field B_{c2} , and $F_{p,max}$ is proportional to $B_{c2}^{2.5}$.⁷ Another potential reason is that the pinning function F_p changes its form as the pinning mechanism switches, as explained by Dew-Hughes' theory.¹⁶ The 12 T layer J_c of sample C is around 6.1 kA/mm². However, a fully reacted Ti doped strands can have a B_{irr} of ~ 25 T.⁵ With such a B_{irr} , we estimate that the 12 T layer J_c might reach ~ 10 kA/mm². It is worth noting that a secondary benefit that the shift of the F_p - B curve to higher field brings is a lower J_c at low field, which benefits the low field stability.¹⁷

In summary, this work explores the way to apply the internal oxidation method to Nb₃Sn wires for grain size refinement. It was shown that SnO₂ powder can be used as oxygen source, but must be positioned in a way that no Cu blocks the path of oxygen to Nb-Zr alloy. This led to the fabrication of composite C, which, when reacted at 650 °C, achieved an average grain size of ~ 43 nm as well as a shift of the $F_{p,max}$ to $\sim 0.3B_{irr}$. It is possible that lowering the reaction temperature to 625 °C would lead to smaller grain size with the peak of F_p - B curve shifting to even higher fields. Beyond this, it is also of interest to use higher Zr contents to see if grain sizes can be reduced even further and to repeat this work with samples with Ti additions via Sn-Ti alloy for B_{irr} optimization. In light of the results obtained, we anticipate that this approach could lead to substantial improvement in the performance of Nb₃Sn conductors at both high and low fields.

This work was funded by the US Department of Energy, Division of High Energy Physics, Grant No. DE-FG02-95ER40900, and a DOE Contract Numbers DE-SC0010312.

¹A. Godeke, A. den Ouden, A. Nijhuis and H.H.J. ten Kate, *Cryogenics* **48**, 308 (2008).

²P. Ferracin, *Adv. Cryog. Eng.* **1218**, 1291 (2010).

³A. K. Ghosh, E. A. Sperry, J. D'Ambra and L. D. Cooley, *IEEE Trans. Appl. Supercond.* **19**, 2580 (2009).

⁴X. Xu, M. D. Sumption, S. Bhartiya, X. Peng and E. W. Collings, *Supercond. Sci. Technol.* **26**, 075015 (2013).

⁵X. Xu, X. Peng, E. Collings, M. D. Sumption, and C. Kovacs, *IEEE Trans. Appl. Supercon.* **24**, 6000904 (2014).

⁶D. Uglietti, V. Abacherli, F. Buta, B. Seeber and R. Flukiger, *Supercond. Sci. Technol.* **19**,1185 (2006).

⁷E.J. Kramer, *J. Appl. Phys.* **44**, 1360 (1973).

⁸D. R. Dietderich and A. Godeke, *Cryogenics* **48**, 331 (2008).

⁹L. E. Rumaner and M. G. Benz, *Metall. Mater. Trans. A* **25**, 213 (1994).

¹⁰B. A. Zeitlin, E. Gregory, J. Marte, M. Benz, T. Pyon, R. Scanlan and D. Dietderich, *IEEE Trans. Appl. Supercon.* **15**, 3393 (2005).

¹¹P. J. Lee, J. R. Ruess and D. C. Larbalestier, *IEEE. Trans. Appl. Supercon.* **7**, 1516 (1997).

¹²P. J. Lee and D. C. Larbalestier, *IEEE Trans. Appl. Supercond.* **15**, 3474 (2005).

¹³W. DeSorbo, *Phys. Rev.* **132**, 107 (1963).

¹⁴C. C. Koch, J. O. Scarbrough and D. M. Kroeger, *Phys. Rev. B* **9**, 888 (1974).

¹⁵C. M. Fischer, M.S. thesis, University of Wisconsin-Madison, Madison, 2002.

¹⁶D. Dew-Hughes, *Philos. Mag.* **30**, 293 (1974).

¹⁷M. D. Sumption, *Adv. Cryog. Eng.* **1219**, 199 (2010).